Available online at www.sciencedirect.com
SCIENCE DIRECT®

Journal of the European Ceramic Society 24 (2004) 2329–2338

www.elsevier.com/locate/jeurceramsoc

Crack-healing and oxidation behavior of silicon nitride ceramics

Keiji Houjou[a], Kotoji Ando[b,*], Sung-Po Liu[c], Shigemi Sato[d]

[a] Yokohama National University, 79-5 Hodogaya, Yokohama, Japan
[b]Department of Energy & Safety Engineering, Yokohama National University, 79-5, Hodogaya, Yokohama, Japan
[c]Department of Mechanical Engineering, Ching–Yun University, 229, Chien-Hsin Rd., Jung-Li, 32049, Taiwan, ROC
[d]NHK Spring Co. Ltd., 3-10 Fukuura Kanazawaku, Yokohama, Japan

Received 10 January 2003; received in revised form 25 June 2003; accepted 6 July 2003

Abstract

Si_3N_4/SiC composite ceramic specimens, made to JIS standard, were sintered and subjected to three-point bending. Semi-elliptical surface cracks of 50–400 μm in diameter were made on the tensile side of each specimen. Crack-healing behavior as a function of environment, temperature, time, and crack size, and oxidation behavior as a function of temperature and time were studied. The main conclusions are as follows: (1) Cracks healed completely in air, but did not heal in Ar gas, N_2 gas nor in a vacuum. (2) This Si_3N_4 ceramic has the ability to heal a crack at temperature from 900 to 1400 °C completely. (3) The maximum surface crack size that can be healed completely was 200 μm in diameter. (4) The activation energies for crack-healing and oxidation were 150 and 131KJ/mol, respectively.

Keywords: Crack-healing; Oxidation behavior; Si_3N_4; Strength

1. Introduction

Silicon nitride has superior strength at elevated temperature however, its fracture toughness is not high, thus it is sensitive to flaws. Some silicon nitride ceramics have the ability to heal a crack.[1–13] If this ability is used on structural components in engineering use, great merits can be anticipated in the following areas: [4,10,11,14] (1) increases in the reliability of structural ceramic components, (2) decreases in the inspection, machining and polishing costs of ceramic components, and (3) reduced maintenance costs and prolongation of the lifetime of ceramic components. To use this healing ability in structural engineering, the authors have already studied the following items on several ceramics systematically: (a) a methodology for evaluating the crack-healing ability,[4–8] (b) the effect of the chemical composition on the crack-healing ability,[7,9] (c) the effect of healing conditions on the strength of the healed-zone, [4,6,8,9] (d) the maximum surface crack size that can be healed completely,[15] (e) knowledge of the high-temperature strength of crack-healed zones,[4–6,9] (f) the crack-healing mechanism,[9,14] (g) assessment of the cyclic fatigue and static fatigue strengths of crack-healed ceramic components,[8,10–12,15–17] (h) a methodology for guaranteeing the reliability of ceramic components,[14,16] and (i) crack-healing behavior under constant or cyclic stress and subsequent strength at the healed temperature (namely in-situ crack-healing ability).[8,10,11,16,18]

As to (b) above, two of the authors sintered many kinds of Si_3N_4, however, they concentrated on the following four kinds of Si_3N_4, because these ceramics showed high performance;[7,9] (1) SNC–Y8, (2) SN–Y8, (3) SNC–Y5A3 and (4) SN–Y5A3. Where, SN, C, Y and A mean that SN = silicon nitride, C = 20 mass% SiC was added to SN, Y8 or Y5 = 8 or 5 mass% Y_2O_3 was added to SN or SNC as a sintering additive, and A3 = 3 mass% alumina was added to SN or SNC as a sintering additive, respectively. In the systematic study, it was found that the crack-healing ability of these Si_3N_4 was SNC–Y8 > > SN–Y8 > SNC–Y5A3 ≅ SN–Y5A3 and SNC–Y8 emerged as having excellent crack-healing ability.[9] The SNC–Y8 can heal cracks only in an air environment but there is no healing in Ar gas, nitrogen gas nor in a vacuum.[4] These facts showed that crack-healing of SNC–Y8 was an oxidation reaction.[4] Thus, the oxidation behavior of the above four Si_3N_4 at

* Corresponding author. Fax: +81-45-339-4024.
E-mail address: andokoto@ynu.ac.jp (K. Ando).

0955-2219/$ - see front matter
doi:10.1016/S0955-2219(03)00645-9

1300 °C up to 2000 h was investigated systematically,[19] where 1300 °C is almost the best temperature for crack-healing of these samples. It was found that the resistance to oxidation was SNC–Y8 > SN–Y8 > > SNC–Y5A3 > SN–Y5A3 and SNC–Y8 exhibited excellent resistance to oxidation at 1300 °C. To understand this paradoxical behavior, SNC–Y5A3 was picked as a sample and the following three research subjects were settled in this paper. (a) crack-healing behavior as a function of crack-healing environment, time, temperature and crack size, (b) oxidation behavior as a function of time and temperature, (c) activation energy for crack-healing and oxidation.

2. Material, specimen and test method

As mentioned above, SNC–Y5A3 was chosen for this study. The silicon nitride powder used in this investigation has the following properties: mean particle size is 0.2 μm, the volume ratio of α-Si_3N_4 is about 95% and the rest is β-Si_3N_4. The SiC powder has 0.27 μm mean particle size.

The sample was prepared using a mixture of silicon nitride powder, 20 mass% SiC, and 5 mass% Y_2O_3, 3 mass% Al_2O_3 as additive powder. To this mixture, alcohol was added and blended thoroughly for 48 h. The mixture was placed into an evaporator to extract the solvent, and then put into a vacuum to produce a dry powder mixture. The mixture was subsequently hot-pressed at 1850 °C and 35 MPa for 1 h in nitrogen gas. The sintered material was then cut into test pieces measuring 3×4×22 mm made according to JIS standard.[20] Only the sample length is changed to 22mm as shown in Fig. 1. A semi-elliptical crack was made at the center of the tension surface of the test piece using a Vickers indenter. The surface crack length (2C) was varied from 50μm to 400μm, by changing the indentation load. The semi-elliptical crack of 2C≒90 μm (aspect ratio≒0.9, the indentation load of about 20N) was chosen as a standard crack in this study, as shown in Fig. 2. The indentation and crack length are shown in Fig. 2 (a). Crack shapes were confirmed on the fracture surfaces of cracked specimens as shown in Fig. 2(b).

The effect of environment on the crack-healing behavior was tested in the following four conditions: in air, vacuum, N_2 gas, and Ar gas. The crack-healing behavior in air was studied systematically to evaluate the activation energy for crack-healing by changing the healing temperature (T_H = 800–1500 °C) and time (t_H :1 h, 10 h, and 100 h). The heating rate was controlled as 10 °C/min, and cooled down in the furnace. To understand the relationship between crack-healing and surface oxidation behavior, the oxidation behavior of crack-healed samples was investigated systematically

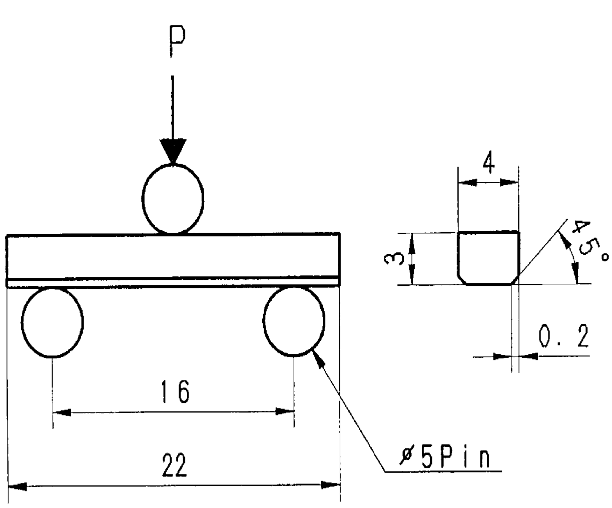

Fig. 1. Three-point loading system and geometry of test specimen; dimensions in mm.

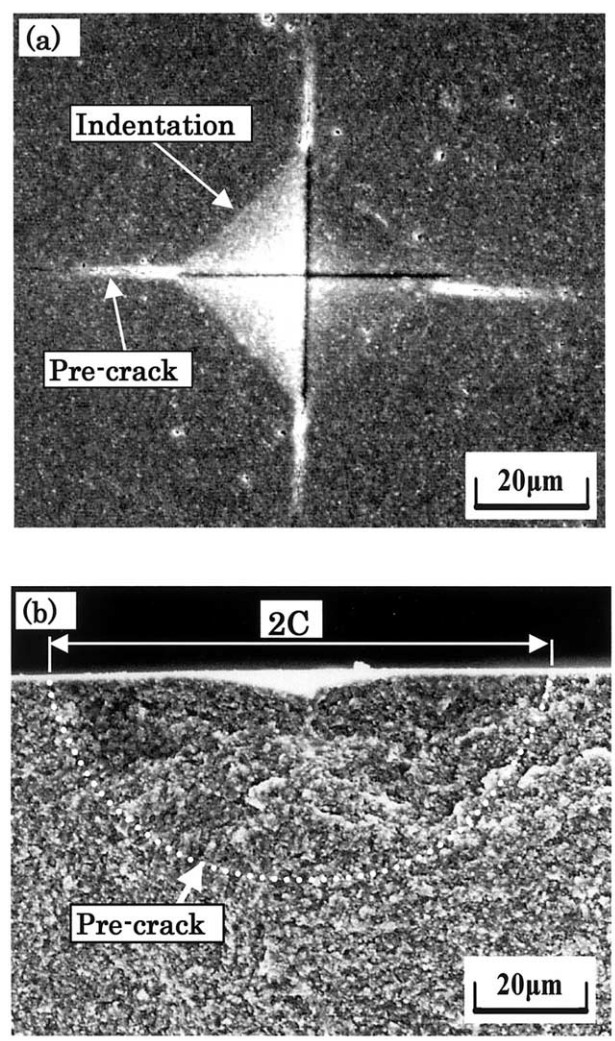

Fig. 2. SEM images of (a) indented crack and (b) crack shape.

using X-ray analyzer and SEM, and the activation energy for the surface oxidation was evaluated.

The maximum crack size that can be healed completely were also studied systematically. The bending strength of the crack-healed specimens was tested at room temperature in air environment using a three-point bending test (bending span = 16 mm), as shown in Fig. 1. The crosshead speed was 0.5 mm/min.

3. Results and discussion

3.1. Effect of healing environment on crack healing behavior

It is very important to define the crack healable environment. Thus, four healing environments were tested: air, vacuum, N_2 gas and Ar gas. One standard crack (2C ≒ 90 μm) is introduced in the sample. The healing temperature (T_H) and healing time (t_H) are 1200 °C and 10 h, respectively. Fig. 3 shows the bending strength (σ_B) of specimens healed in each environment. The contrast between σ_B of smooth specimens (○) and cracked specimens (△) is shown by the left-most column of result. The symbol (*) indicates a specimen that fractured outside the crack healed zone as shown in Fig. 4(b). All samples healed in air recovered σ_B completely, and showed that the cracks were healed completely. One sample fractured from outside the crack healed zone as shown in Fig. 4(b). Fig. 4(c) and (d) show the crack initiation site of Fig. 4(b). Fracture initiated from a small pore. The other two samples were broken into many pieces, so the crack initiation sites could not be found. Specimens healed in vacuum, Ar gas and N_2 gas indicated that the strength recovery was insufficient, and all samples fractured from the crack-healed zone as shown in Fig. 4(a). The average σ_B of the specimens healed in vacuum is 730 MPa, which is a little higher than that of the other two conditions (Ar gas and N_2 gas). This insufficient strength recovery was caused by the removal of residual stress ahead of the crack, that was introduced by Vickers indentation.[21,22] These test results showed that a crack in SNC–Y5A3 can be healed completely only in an air environment similar to SNC–Y8,[4] Al_2O_3/SiC[23] and Mullite/SiC. [24,25] Therefore, it is assumed that the crack-healing is due to oxidation. The estimated crack-healing reactions are the following.[14,19]

$$Si_3N_4 + 3O_2 \rightarrow 3SiO_2 + 2N_2 \quad (1)$$

$$SiC + 2O_2 \rightarrow SiO_2 + CO_2(CO) \quad (2)$$

$$2SiC + Y_2O_3 + 4O_2 \rightarrow Si_2Y_2O_7 + 2CO_2(CO) \quad (3)$$

On the other hand, it was already shown that the monolithic Al_2O_3 specimen could recover its strength over 1450 °C, under the above four environments.[23] In this case, oxidation is not necessary, because this strength recovery was caused by re-sintering at high temperature.[23] Surface of specimens healed in each environment was analyzed with XRD. The only specimen healed in air diffracts the SiO_2 peaks intensely.

3.2. Effect of healing temperature and time on crack-healing behavior

Crack-healing behavior depends on both healing temperature (T_H) and time (t_H).[24,26] To investigate this relationship, 15 kinds of healing conditions were tested. The test results are shown in Fig. 5. The bending strength σ_B of smooth (○) and cracked (△) specimens are compared in the left-most column. The (*) mark indicates that fracture occurred from outside the crack-healed zone, as mentioned before in Fig. 4(b). The symbol (◆) indicates the σ_B obtained by healing time $t_{H=}$1 h at each healing temperatures. Note that σ_B does not recover up to T_H = 1100 °C, but it recovers considerably at T_H = 1200 °C and 1300 °C. However, when considering that many fractures occurred from a pre-crack, as shown in Fig. 4(a), the recovery is not sufficient. On the other hand, at T_H = 1400 °C, the average σ_B of a healed specimen is higher than that of a smooth specimen. Moreover, all of the specimens fractured from outside the healed zone, as shown in Fig. 4 (b). At 1500 °C, σ_B decreases slightly. In conclusion, the desirable crack-healing temperature for $t_{H=}$1 h is $T_{H=}$1400 °C. In the same way, the desirable crack-healing temperature conditions for t_H = 10 h (□) and t_H = 100 h (●) are T_H = 1100–1300 °C and T_H = 900–1100 °C, respectively.

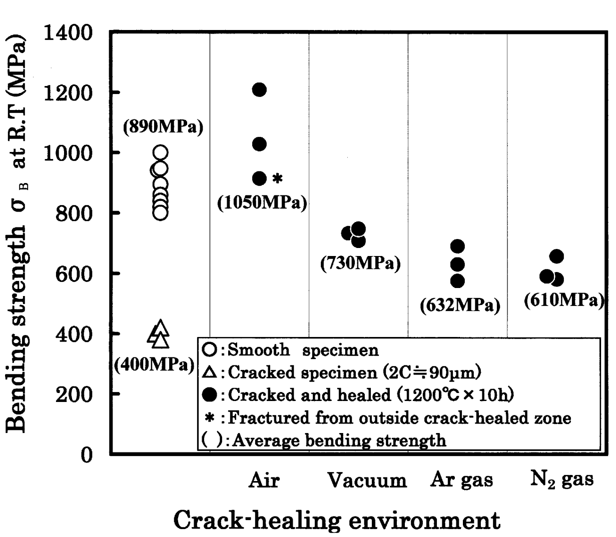

Fig. 3. Effect of crack-healing environment on the strength recovery behavior.

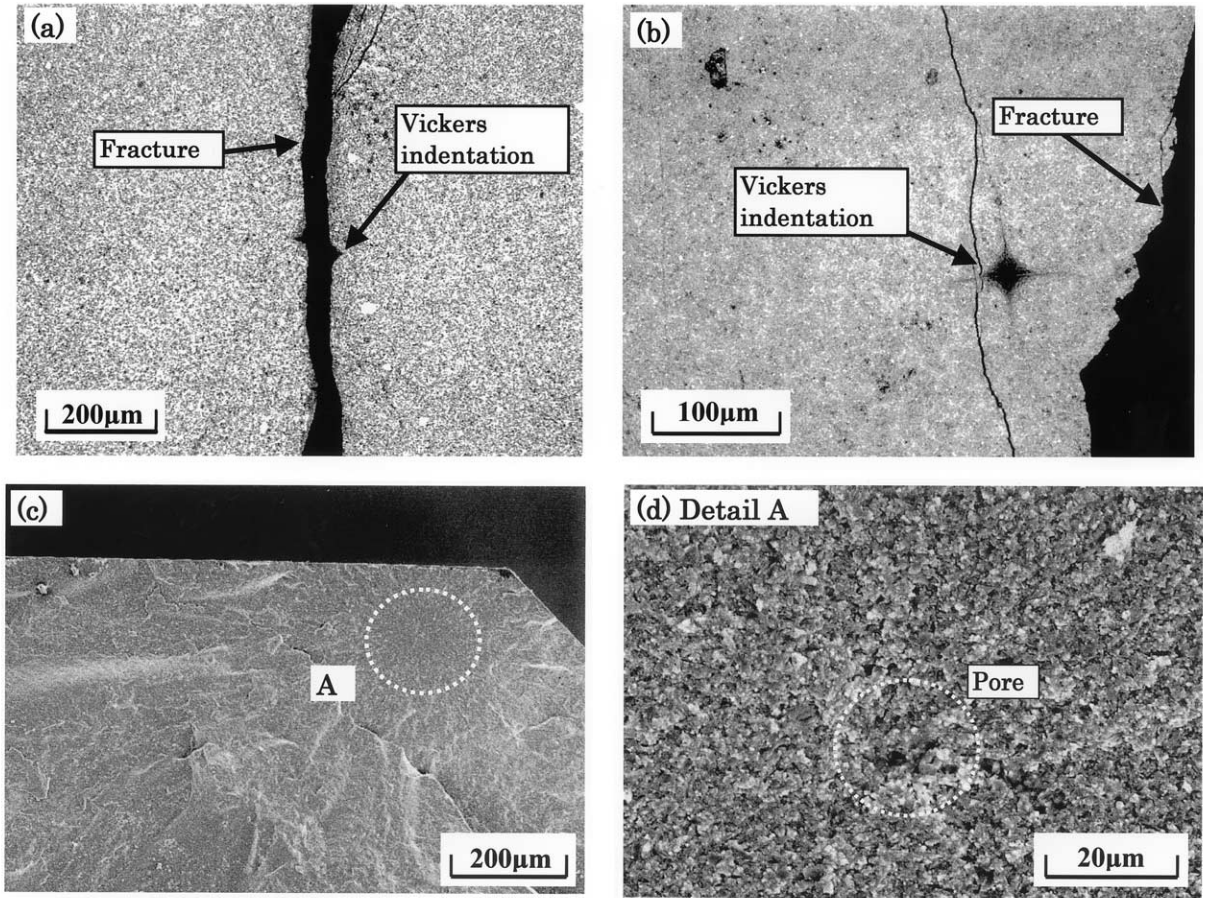

Fig. 4. Fracture pattern of crack-healed sample: (a) crack initiated from crack-healed zone, $T_H = 900$ °C, $t_H = 100$ h, $\sigma_B = 896$ MPa, (b) crack initiated from the outside of crack-healed zone, $T_H = 1100$ °C, $t_H = 100$ h, $\sigma_B = 889$ MPa, (c) fracture surface of sample (b), (d) in detail of (c).

To understand the effect of crack-healing conditions on σ_B, SEM observation and X ray analysis are applied to the surface of healed samples. Fig. 6 shows the SEM images and XRD profiles. Fig. 6 (a) shows $T_H = 800$ °C, $t_H = 100$ h. Under this condition, the crack was not healed at all, as shown by the symbol (●) in Fig. 5. The surface is almost smooth, as shown in the SEM image. When looking at the XRD profile, only β-Si_3N_4 and β-SiC peaks diffract the same as non-healed specimen. Other crystalline products are not found. Fig. 6(b) shows $T_H = 1200$ °C, $t_H = 10$ h condition. The average σ_B of samples healed in this condition has the highest value. As shown in the SEM image, very small particles are observed on the surface. As the results of XRD analysis, this product consists of SiO_2 and a small amount of $Y_2Si_2O_7$. As mentioned before, the production of crystalline SiO_2 has a large effect on σ_B and the fatigue strength at elevated temperatures, so the healing condition ($T_H = 1200$ °C, $t_H = 10$ h) was selected as the standard healing condition for this material.

Notably, as shown in Fig. 6(c) $T_H = 1200$ °C, $t_H = 100$ h, the bending strength decreases considerably. When looking at the SEM image, the surface is very rough, and many holes like craters of about 10 μm in diameter are observed. While Si_3N_4 and SiC are oxidized, N_2 gas, CO or CO_2 gas are produced, as represented in Eqs. (1)–(3). These holes seem to be made by the produced gas. As the results of XRD, large amounts of SiO_2 and $Y_2Si_2O_7$ are detected. Therefore, it is clear that the decrease of σ_B is responsible for the over oxidation of base material. In Fig. 6(d) $T_H = 1300$ °C, $t_H = 100$ h, very large crystals of $Y_2Si_2O_7$ are observed. The oxidation reaction became more intense. From the XRD results, the peak of $Y_2Si_2O_7$ is diffracting remarkably, and it has also exceeded the Si_3N_4 peaks, while the SiO_2 peak is slight. This oxidation reaction reduces the σ_B, because of the production of many pits inside the base material.[19] Considering the above-mentioned facts, it can be easily understood that the conditions and products on the surface have a large effect on the σ_B of crack-healed sample.

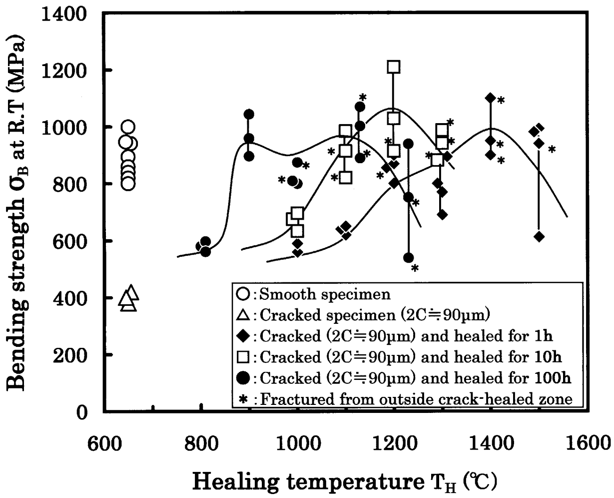

Fig. 5. Effect of crack-healing temperature (T_H) and time (t_H) on the crack-healing behavior.

3.3. Activation energy for the crack-healing

The crack-healing behavior depends on both the healing temperature and the healing time, as mentioned in Section 3.2. And, the crack-healing is caused by the oxidation as shown in Eqs. (1)–(3). The oxidation rates of Eqs. (1)–(3) obey Arrhenius law. Thus, it is expected that the crack-healing rate obeys the Arrhenius law. Moreover, if the minimum crack-healing time for sufficient strength recovery were expressed as a function of temperature, it would be very convenient for engineering use. Then, whether the crack-healing rate of this sample obeys Arrhenius law or not was investigated.

From Fig. 5, the lowest temperatures (T_H) that the average σ_B of the crack-healed sample exceeded the average σ_B of smooth specimens were determined. For each healing time ($t_{HMin}=1$, 10, 100 h), T_H was determined and the t_{HMin} versus T_H relationship were plotted in an Arrhenius graph as shown in Fig. 7. In short, $T_H=1400$ °C is for $t_{HMin}=1$ h, $T_H=1100$ °C is for $t_{HMin}=10$ h, and $T_H=900$ °C is for $t_{HMin}=100$ h, where the minimum healing time for the complete strength recovery is denoted as (t_{HMin}). The Arrhenius plots of four kinds of ceramics were also shown in Fig. 7. Symbol (●) indicates the SNC–Y5A3, used for this study. Symbols (▲), (■) and (◆) show the results for SNC–Y8,[27] Al_2O_3/SiC[24] and mullite/SiC,[25] respectively. Crack size of these three materials are 2C ≒100μm, and they are healed in an air environment. Symbol (↑) shows that the crack can be healed within this time period. With respect to these four kinds of ceramics, both (T_H^{-1}) and ($1/t_{HMin}$) are in the good proportional relation. Therefore, the crack-healing behavior of these ceramics may be described by the Eq. (4).[24,26]

$$(1/t_{HMin}) = A_H \cdot \exp(-Q_{aH}/R \cdot T_H) \qquad (4)$$

Where A_H is proportionality constant (h^{-1}), Q_{aH} is the activation energy for crack-healing (kJ/mol), R is a gas constant (kJ/mol·K) and T_H is the absolute temperature of the healing (K). The Q_{aH} and A_H of each ceramics are shown in Table 1. The sensitivity of crack-healing rate on temperature increases with increasing Q_{aH}. The calculated Q_{aH} value of SNC–Y5A3 (●) is 150 (kJ/mol). This Q_{aH} is almost equal to the activation energy of SiC (135KJ/mol) for oxidation from 1000–1400 °C.[27] The value for SNC–Y5A3 is rather smaller than that of SNC–Y8 (277 kJ/mol).[26] These results of Q_{aH} indicate that the crack-healing behavior of SNC–Y8 is more sensitive to the healing temperature (T_H) than that of SNC–Y5A3. Crack-healing in mullite/SiC is most sensitive to temperature,[26] and its activation energy (Q_{aH}) is 413 (kJ/mol). The t_{HMin} of SNC–Y8 is the shortest for the temperature range (900–1300 °C), thus it can be concluded that SNC–Y8 (▲) is a very interesting material in terms of crack-healing ability. The minimum crack-healing time (t_{HMin}) for the sufficient strength recovery can be calculated as a function of crack-healing temperature using Eq. (4) and the activation energy (Q_{aH}).

3.4. Oxidation behavior

The oxidized layer thickness (T_O) on the sample surfaces were measured, using an SEM, as a function of crack-healing temperature and time, and shown in Fig. 8. Fig. 8(a) shows the T_O on the fracture surface under the condition of $T_H=1100$ °C, $t_H=100$ h. The oxidized zone looks like a glassy phase, so it can be distinguished from base material easily. The T_O is almost uniform and about 1 μm in thickness. Fig. 8(b) is the SEM image of the fracture surface, and Fig. 8(c) is the SEM image of the polished surface. The T_O was measured systematically using these SEM images, and the relationship between the healing time (t_H) and oxidized layer thickness (T_O) is shown in Fig. 9. The oxidation behavior of four kinds of Si_3N_4 followed parabolic-law kinetics up to 2000 h at 1300 °C.[19] Thus following parabolic-law was assumed for this case.

Table 1
The activation energy Q_{aH} and proportionality constant A_H for the crack-healing

	Sample name	Q_{aH} (kJ/mol)	A_H (h^{-1})
1	SNC–Y5A3	150	4.9×10^4
2	SNC–Y8	277	4.2×10^{11}
3	Al_2O_3/SiC	334	1.7×10^{11}
4	Mullite/SiC	413	5.4×10^{13}

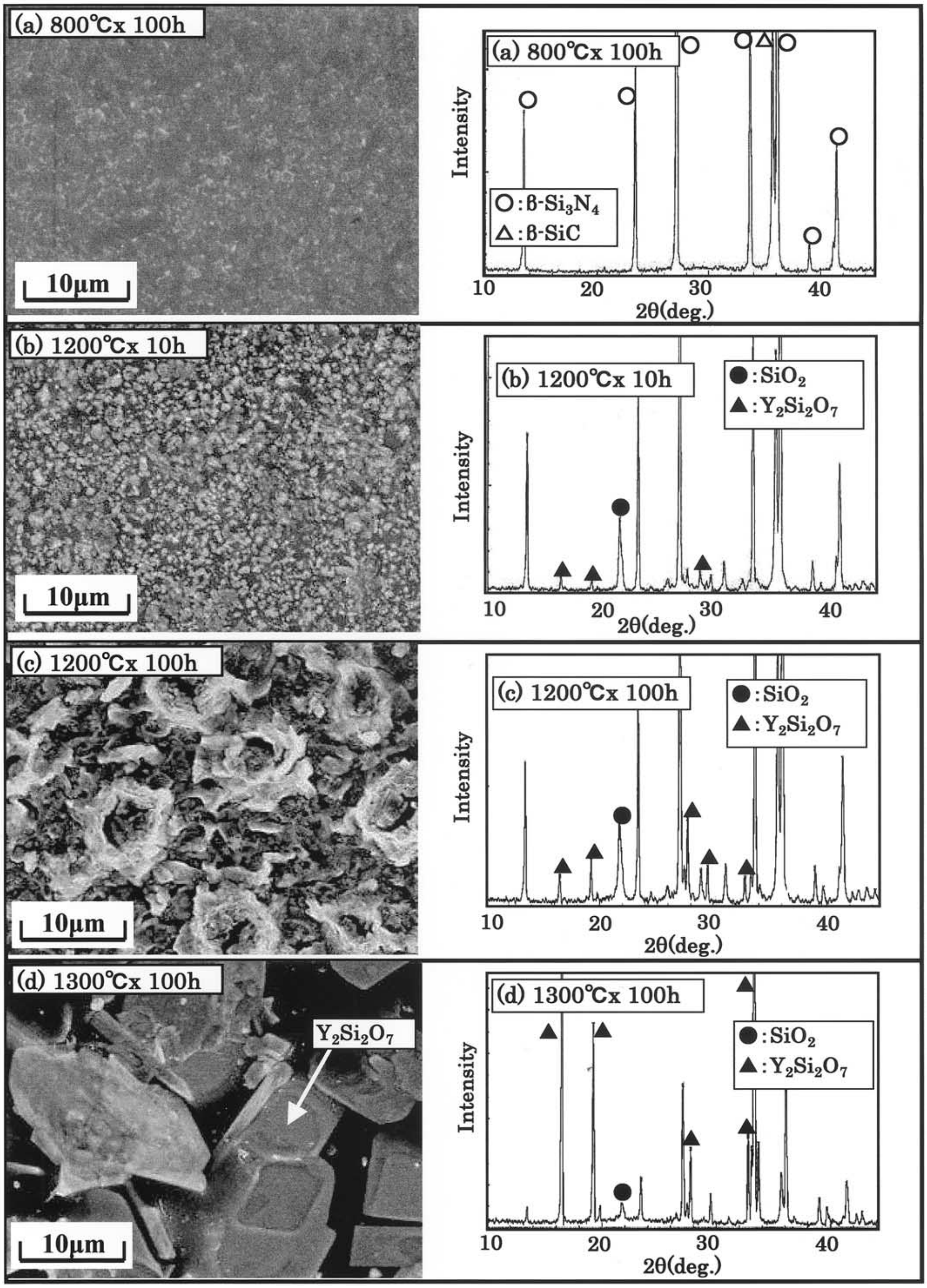

Fig. 6. SEM images and XRD results of healed sample surface: (a) $T_H = 800$ °C, $t_H = 100$ h, (b) $T_H = 1200$ °C, $t_H = 10$ h, (c) $T_H = 1200$ °C, $t_H = 100$ h, (d) $T_H = 1300$ °C, $t_H = 100$ h.

$$T_O = k_{OX} \cdot t_H^{(1/2)} \tag{5}$$

Where, T_O is the thickness of the oxidized layer (μm), t_H is the crack-healing time (namely oxidation time; h) and k_{OX} is a oxidation rate constant. The k_{OX} of $T_H = 1300$ °C (◆) is the largest one, having a value of 0.6 (μm/h$^{1/2}$). The k_{OX} of $T_H = 1200$ °C (●) is one-half of $T_H = 1300$ °C and the k_{OX} of $T_H = 1100$ °C (■) is one-fourth that of $T_H = 1300$ °C. The solid lines are drawn using Eq. (5) and the rate constant (k_{ox}) indicated in the graph.

By the same method of crack-healing activation energy, the activation energy (Q_{aO}) and proportionality constant (A_O) for the oxidation were evaluated. The relationship between healing temperature (T_H) and oxidation rate constant (k_{OX}) are plotted in an Arrhenius

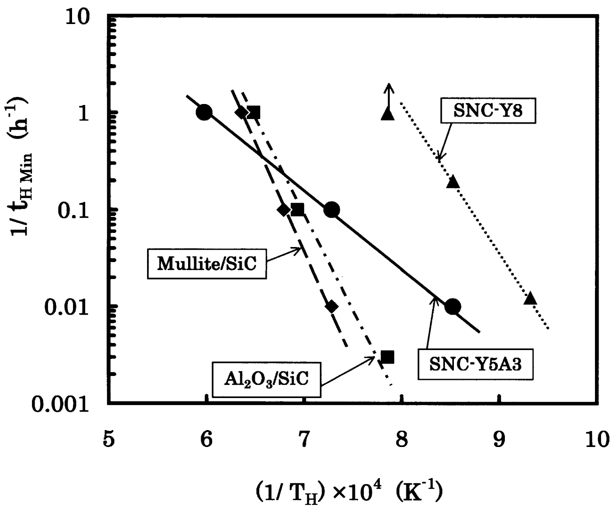

Fig. 7. Arrhenius plots of crack-healing behavior of four kinds of ceramics.

graph, as shown in Fig. 10. SNC–Y5A3 is denoted by the symbol (●), and SNC–Y8 by the symbol (▲). The activation energies (Q_{aO}) of SNC–Y5A3 and SNC–Y8 are 131 kJ/mol and 24 kJ/mol, respectively. The values of Q_{aO} and A_O are shown in Table 2. It can be seen that the oxidation rate of SNC–Y5A3 is considerably larger than that of SNC–Y8. However the crack-healing ability of SNC–Y5A3 is slower than that of SNC–Y8, as shown in Fig. 7. It is very interesting that the orders of activation energy of both samples for crack-healing and oxidation are reversed. If one focused on the both behaviors at 1100 °C, the oxidized layer thickness of SNC–Y5A3 for 1 h is larger than that of SNC–Y8, on the contrary, the minimum crack-healing time for the sufficient strength recovery of SNC–Y5A3 is longer than that of SNC–Y8. The exact answer to this paradoxical behavior is very difficult, however the possible reasons for the behavior are summarized as follows; (1) oxygen can be supplied sufficiently on the sample surface, however, oxygen cannot be supplied sufficiently to the crack inside. Thus there is a possibility that the oxidation mechanisms are different between the sample surface and crack surface. (2) More oxygen products are formed on the SNC–Y5A3 surface than that of SNC–Y8, and these oxygen products probably disturb the supply of oxygen into the crack surface. (3) The roughness of the crack surface of both sample are different, the roughness of SNC–Y5A3 is larger than that of SNC–Y8, thus the thickness of the oxidized layer required for sufficient crack-healing of SNC–Y5A3 is larger than that of SNC–Y8. (4) The materials for crack-healing are somewhat different in both samples, thus the thickness of the oxidized layer required for sufficient crack-healing of both samples are different.

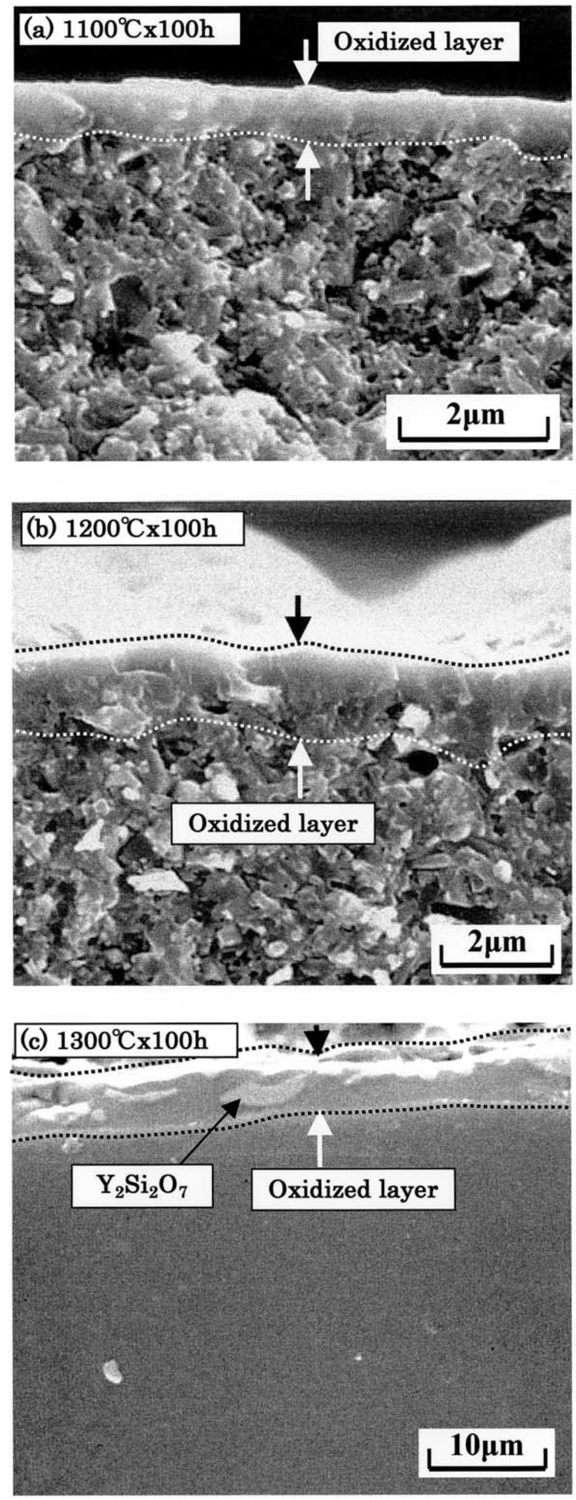

Fig. 8. SEM images of oxidized layer: (a) $T_H = 1100$ °C, $t_H = 100$ h, (b) $T_H = 1200$ °C, $t_H = 100$ h, (c) $T_H = 1300$ °C, $t_H = 100$ h.

3.5. The maximum crack size to be healed completely

Surface cracks (2C = 90–300 μm) were introduced, and healed under the standard condition ($T_H = 1200$ °C $t_H = 10$ h in air). Subsequently the bending test was

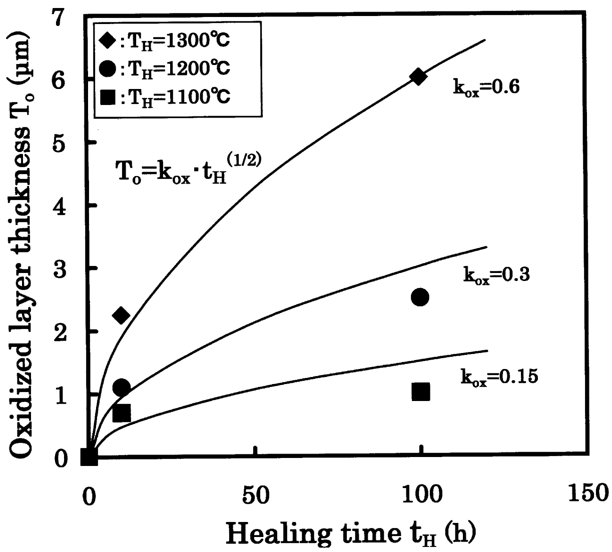

Fig. 9. Relationship between crack-healing time (t_H) and thickness of oxidized layer (T_o).

Table 2
The activation energy Q_{aO} and proportionality constant A_O for the oxidation

	Sample name	Q_{aO} (kJ/mol)	A_O (μm/h$^{1/2}$)
1	SNC–Y5A3	131	1.5×10^4
2	SNC–Y8	24	0.98

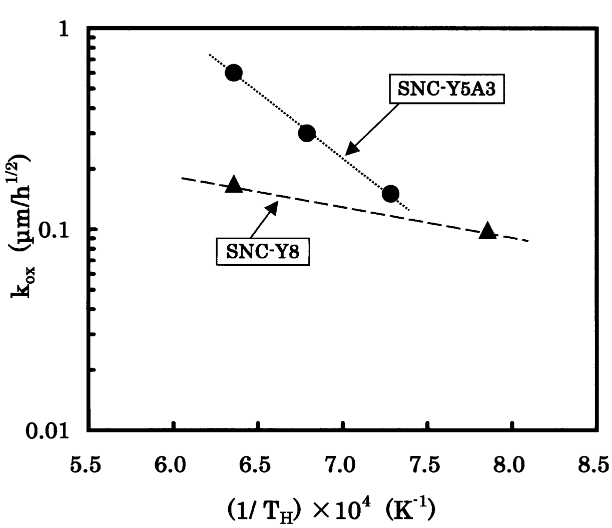

Fig. 10. Arrhenius plots of the oxidation behavior of two kinds of silicon nitride ceramics.

carried out at room temperature. The relationship between the crack length (2C) and bending strength (σ_B) is shown in Fig. 11. The symbols (○) and (△) indicate the σ_B of smooth specimens and cracked specimens (non-healed), respectively. Moreover the symbols (◇) show the σ_B of specimens which were cracked and annealed in N_2 gas environment. The σ_B of annealed sample is higher by about 150–200 MPa than that of non-healed specimens (△) because of annealing of the tensile residual stress ahead of crack tip. The σ_B (●) of crack-healed sample regains the same level σ_B as the smooth specimens (○), when 2C is smaller than 200 μm. But the σ_B decreases suddenly, when 2C is over 200 μm. Therefore, the maximum crack size to be healed completely is 2C = 200 μm. SNC–Y8, Al_2O_3/SiC, mullite/SiC, and SiC were also tested in the same way. Table 3 lists the maximum crack size to be healed completely for five kinds of structural ceramics.[15,23,26] Only SiC could heal a large crack of 2C = 450 μm by itself.[28] The other materials can heal a crack up to 2C = 200 μm, completely.

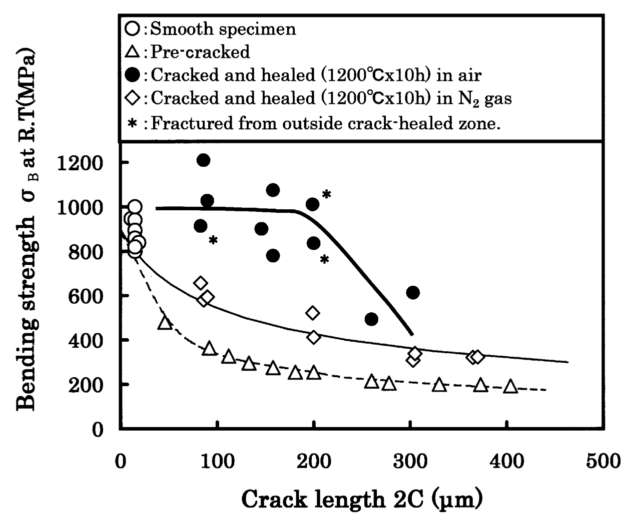

Fig. 11. Relationship between crack length 2C and bending strength σ_B at RT.

Table 3
The maximum crack size that can be healed, of five different ceramics

	Sample name	Maximum crack size (μm)
1	SNC–Y5A3	200
2	SNC–Y8	200
3	Al_2O_3/SiC	200
4	Mullite/SiC	200
5	SiC	450

4. Conclusions

Using silicon nitride (SNC–Y5A3), a fundamental study on crack-healing and oxidation behavior was carried out. A crack was introduced; also the effect of healing temperature and time on the bending strength of healed samples was investigated. Moreover, the effect of crack size on the crack-healing behavior was investigated. The main conclusions are as follows:

1. This ceramic could heal a crack in an air environment, but could not heal in N_2 gas, Ar gas nor in a vacuum environment. Crack-healing needed the oxygen in air to produce SiO_2.
2. The crack-healing behavior was studied as a function of crack-healing temperature and time, systematically. The activation energy for crack-healing (Q_{aH}) was evaluated as 150 kJ/mol. The value was compared with Q_{aH} of other ceramics, and it was shown that this material has the relatively low value.
3. The surface oxidation behavior of the crack-healed sample was studied systematically, and the activation energy for the oxidation was evaluated as $Q_{a0} = 131$ kJ/mol. It was found that this value is much greater than that of SNC–Y8 ceramics.
4. The maximum crack size that could be healed completely was studied systematically, and the maximum crack was found to be a $2C \approx 200$ μm surface crack of 0.9 aspect ratio. The value was almost equal to that of other ceramics except SiC for which the 2C was 450 μm.

Acknowledgements

This study was supported by Grant-in-Aid in scientific research of Japan Ministry of Education, Basic Research Category (C)(2) No.13650076 of the term from 2001 to 2002. Authors show their sincere thanks for the support. Dr. Liu also shows his sincere thanks to International Educational Organization of Japan for the scholarship to study at Yokohama National University.

References

1. Choi, S. R. and Tikara, V., Crack-healing behavior of hot-pressed silicon nitride due to oxidation. *Scripta. Metall. Mater.*, 1992, **26**, 1263–1268.
2. Ogasawara, T., Hori, T. and Okada, A., Thereshold stress intensity for oxidative crack healing in sintered silicon nitride. *J. Mat. Sci. Lett.*, 1994, **13**, 404–406.
3. Zhang, Y. Z., Edwards, L. and Plumbridge, W. J., Crack healing in a silicon nitride ceramics. *J. Am. Ceram. Soc.*, 1998, **81**, 1861–1868.
4. Ando, K., Ikeda, T., Sato, S., Yao, F. and Kobayashi, Y., A preliminary study on crack healing behaviour of Si_3N_4/SiC composite ceramics. *Fatigue Fract. Engng. Mater. Struct*, 1998, **21**, 119–122.
5. Ando, K., Sato, S., Kobayashi, Y. and Chu, M. C., Crack healing behaviour of Si_3N_4 ceramics and it's application to structural integrity. In *Fracture From Defects, ECF-12* ed. M.W. Brown, E.R. de los Rios and K.J. Miller. Engineering Materials Advisory Services, 1998, pp. 497–502.
6. Ando, K., Chu, M. C., Sato, S., Yao, F. and Kobayashi, Y., The study on crack healing behaviour of silicon nitride ceramics. *Jpn. Soc. Mech. Eng.*, 1998, **64-623**, 1936–1942 (in Japanese).
7. Chu, M. C., Ando, K., Hirasawa, T., Sato, S. and Kobayashi, Y., Crack Healing behaviour of silicon nitride ceramics (effect of sintering additives and sintering powder.). *High Pressure Institute of Japan*, 1998, **36-2**, 82–89 (in Japanese).
8. Ando, K., Chu, M. C., Yao, F. and Sato, S., Fatigue strength of crack-healed Si_3N_4/SiC composite ceramics. *Fatigue Fract. Eng. Mater. Struct*, 1999, **22**, 897–903.
9. Ando, K., Chu, M. C., Kobayashi, Y., Yao, F. and Sato, S., Crack healing behavior and high temperature strength of silicon nitride ceramics. *Jpn. Soc. Mech. Eng.*, 1999, **65-633**(A), 1132–1139 (in Japanese).
10. Ando, K., Houjou, K., Chu, M. C., Takeshita, S., Takahashi, K. and Sato, S., Crack-healing behavior of Si_3N_4/SiC ceramics under stress and fatigue strength at the temperature of healing (°C). *J. Eur. Ceram. Soc.*, 2002, **1000**, 22 1339-1346.
11. Takahashi, K., Kim, B. S., Chu, M. C., Saito, S. and Ando, K., Self crack-healing behavior under stress of silicon nitride ceramics and resultant strength at the crack-healed temperature. *Jpn. Soc. Mech. Eng.*, 2002, **68-761**(A), 1063–1070 (in Japanese).
12. Yao, F., Ando, K., Chu, M. C. and Sato, S., Crack-healing behavior, high-temperature and fatigue strength of SiC-reinforced silicon nitride composite. *J. Mat. Sci. Lett.*, 2000, **12**(19), 1081–1084.
13. Lube, T., Improvement of the strength of silicon nitride by aging. In *Fracture Mechanics of Ceramics*, ed. Bradt R.C. et al. Kluwer Academic/Plenum Publishers. Vol. 13, 2002, pp. 151–157.
14. Ando, K., Shirai, Y., Nakatani, M., Kobayashi, Y. and Sato, S., (Crack-healing + Proof test): a new methodology to guarantee the structural integrity of a ceramics component. *J. Eur. Ceram. Soc.*, 2002, **22**, 121–128.
15. Ando, K., Furusawa, K., Chu, M. C., Hanagata, T., Tsuji, K. and Sato, S., Crack-healing behavior under stress of mullite/SiC ceramics and resultant fatigue strength. *J. Am. Ceram.Soc.*, 2001, **84**(9), 2073–2078.
16. Ando, K., Chu, M. C., Matsushita, S. and Sato, S., Effect of crack-healing and proof-testing procedures on fatigue strength and reliability of Si_3N_4/SiC composites. *J. Eur. Ceram. Soc.*, 2003, **23**, 977–984.
17. Yao, F., Ando, K., Chu, M. C. and Sato, S., Static and cyclic behaviour of crack-healed Si_3N_4/SiC composite ceramics. *J. Eur. Ceram. Soc.*, 2001, **21**, 991–997.
18. Ando, K., Takahashi, K., Nakayama, S. and Saito, S., Crack-healing behavior of Si_3N_4/SiC ceramics under cyclic stress and resultant fatigue strength at the healing temperature. *J. Am. Ceram. Soc.*, 2002, **85**(9), 2268–2272.
19. Houjou, K., Hirai, K., Ando, K., Chu, M. C., Matushita, S. and Sato, S., Effect of sintering additives on the oxidation behavior of Si_3N_4 at 1300°. *Jpn. Soc. Mater. Sci.*, 2002, **51-11**, 1235–1241 (in Japanese).
20. JIS 1061, Testing method for fracture toughness of high performance ceramics. Japan Standard Association, 1993.
21. Marshall, D. B. and Lawn, B. R., Residual stress effects in sharp contact cracking. *J. Material Science*, 1979, **14**, 2001–2012.
22. Kim, B. A., Meguro, S., Ando, K. and Ogura, N., Study on

fracture toughness of silicon nitride ceramics. *High Pressure Institute of Japan*, 1990, **28**, 218–228 (in Japanese).

23. Kim, B. S., Ando, K., Chu, M. C. and Saito, S., Crack-healing behavior of alumina and strength of crack-healed member. *Jpn. Soc. Mater. Sci.*, 2003, **52-6**, 667–673 (in Japanese).
24. Furusawa, K., Furumachi, N., Takahashi, K., Saito, S., and Ando, K., In situ crack-healing behavior of mullite/SiC composite ceramics. *Jpn. Soc. Mater. Sci.*, accepted for publication (in Japanese).
25. Ando, K., Chu, M. C., Tuji, K., Hirasawa, T., Kobayashi, Y. and Sato, S., Crack healing behavior and high temperature strength of mullite/SiC composite ceramics. *J. Eur. Ceram. Soc.*, 2002, **22**, 1313–1319.
26. Ando, K., Furusawa, K., Takahashi, K., Chu, M. C. and Sato, S., Crack-healing behavior of structural ceramics under constant and cyclic stress at elevated temperature. *J. Ceram. Soc. Jpn.*, 2002, **110**(8), 741–747.
27. Nanri, H. and Nagasoe, A., Effect of small amount of iron impurity on oxidation of powder SiC. *Taikabustu*, 1999, **51**, 650–655 (in Japanese).